

Origin of room-temperature ferromagnetism in Mn doped semiconducting CdGeP₂

Priya Mahadevan and Alex Zunger

National Renewable Energy Laboratory, Golden-80401

(October 26, 2018)

CdGeP₂ chalcopyrites doped with Mn have been recently found to exhibit room temperature ferromagnetism. Isovalent substitution of the Cd site is expected, however, to create *antiferromagnetism*, in analogy with the well-known CdTe:Mn (d^5) case. However, chalcopyrite semiconductors exhibit low-energy intrinsic defects. We show theoretically how ferromagnetism results from the interaction of Mn with hole-producing intrinsic defects.

Spintronics [1] - the use of spin rather than charge in electronics - calls for room-temperature ferromagnetism in a semiconductor. While there have been several attempts to dope semiconductors with transition metal atoms [2], most of them did not show magnetic ordering. The dopant of choice here [3] is Mn⁰ (d^5s^2), being formally Mn²⁺ (d^5) when substituting a divalent cation, and Mn³⁺ (d^4) when replacing a trivalent cation. Mn on the divalent cation site of II-VI semiconductors is attractive because of the significant solubility of the isovalent Mn²⁺, but this produces antiferromagnetism [4]. The reason is that in a ferromagnetic arrangement all $3d$ spin-up orbitals are occupied so there is no empty orbital on a neighboring Mn atom for the electron from one Mn atom to hop onto. Therefore an antiferromagnetic arrangement of spins at neighboring Mn sites is favored. The III-V compounds doped with Mn would have been suitable candidates for ferromagnetism as these systems are known [5] to have holes ($d^4 \rightarrow d^5 + \text{hole}$) when Mn³⁺ substitutes the trivalent cation site. However, the ferromagnetic transition temperature (T_c) in these compounds is limited by the fact that Mn³⁺ has low solubility [3], and above a critical concentration ($\sim 8\%$ in GaAs) tends to phase separate. This was not a limitation while doping the II-VI semiconductors. Recently, Medvedkin *et al.* [6] came up with the novel idea of obtaining both high solubility and high T_c in a semiconductor: replacing Cd sites in the chalcopyrite CdGeP₂ with Mn atoms. Although CdGeP₂ is isovalent to the III-V compounds [7] (the average valence of Cd and Ge is a group III element), a large amount ($\sim 50\%$ at the surface) of Mn could be doped into this system, resulting in ferromagnetism in a semiconductor at the unprecedented high temperature ($T_c=320$ K) [6]. However, the existence of ferromagnetism in CdGeP₂:Mn is surprising since, as explained above, replacement of a divalent site by Mn²⁺ (d^5) is known [4] to give rise to an antiferromagnetic interaction between the Mn atoms. Indeed, recent electronic structure calculations [9] found that Mn doped CdGeP₂ was antiferromagnetic, just like Mn doped CdTe [8]. We show here that Mn doping in CdGeP₂ can produce stable ferromagnetism. This hitherto unexplored unusual form of ferromagnetism results from the interaction of a magnetic ion such as Mn with holes produced by *intrinsic defects*. The central point is that chalcopyrite semicon-

ductors are known [10] to be stabilized by certain intrinsic defects such as cation (Cd,Ge) vacancies, vacancy-antisite pairs and the presence of hole-producing defects which could result in ferromagnetism being favored even when Mn dopes the Cd site. The theoretical challenge is to identify the hole-producing defects that form stable complexes with substitution. In this work we have calculated the formation energies of various kinds of defects and predicted the conditions favoring the substitution of Cd sites and Ge sites by Mn. From this we infer that ferromagnetism is induced by holes generated in structures resulting from the simultaneous substitution of both Cd and Ge sites or the substitution of only the Ge sites with Mn. This offers a novel design principle for obtaining both high Mn solubility and high- T_c ferromagnetism due to defect-induced hole production in semiconducting systems.

We first calculated the formation energies of intrinsic point defects such as a vacancy at a Cd site (V_{Cd}), a vacancy at a Ge site (V_{Ge}) and a Ge antisite on Cd (Ge_{Cd}), finding the energetically stablest defects. Then we calculate formation energies for Mn substituting a Cd site (Mn_{Cd}) and a Ge site (Mn_{Ge}). Finally we deduce which of the many possible complexes among such single point defects and Mn would have simultaneously low formation energy (hence, high concentration) and create hole states (therefore coupling the Mn atoms ferromagnetically).

We performed plane-wave pseudopotential [11–13] calculations with isolated defects/Mn atoms introduced into 64 atom supercells of CdGeP₂. The lattice parameters of these supercells were fixed at the theoretically calculated values for CdGeP₂: $a=5.81$ Å and $c=10.96$ Å ; while the atomic positions were relaxed. The formation energy for a defect comprising of atoms α in the charge state q was computed using the expression [10]

$$\Delta H_f(\alpha, q) = E(\alpha) - E(0) + \sum_{\alpha} n_{\alpha} \mu_{\alpha}^a + q(E_{VBM} + \epsilon_f) \quad (1)$$

where $E(\alpha)$ and $E(0)$ are the total energies of the supercell with and without defect α . n_{α} is the number of each defect atom; $n_{\alpha} = -1$ if an atom is added, while $n_{\alpha} = 1$ if an atom is removed. μ_{α}^a is the absolute value of the chemical potential of atom α . Since the formation energies are conventionally defined with respect to the elemental solid (s), we express μ_{α}^a as the sum of a

component due to the element in its most commonly occurring structure μ_α^s , and an excess chemical potential μ_α i.e $\mu_\alpha^a = \mu_\alpha^s + \mu_\alpha$. Here μ_α^s for P, Ge, Mn and Cd are the total energies evaluated for the fully-optimised elemental solids in the observed crystal structures [14]. If $\Delta H_f(\text{CdGeP}_2)$ is the formation energy of CdGeP_2 , then μ_{Cd} and μ_{Ge} are determined by

$$\mu_{\text{Cd}} + \mu_{\text{Ge}} + 2\mu_{\text{P}} \leq \Delta H_f(\text{CdGeP}_2) \quad (2)$$

Furthermore, $\mu_{\text{Cd}} \leq 0$; $\mu_{\text{Ge}} \leq 0$, because otherwise the elemental solids will precipitate. The presence of other intervening binary phases, however, further restricts the values of μ_{Cd} and μ_{Ge} : One must solve Eq. (2) along-with the constraints placed by the formation energies $\Delta H_f(\text{Cd}_3\text{P}_2)$ and $\Delta H_f(\text{GeP})$ of Cd_3P_2 and GeP

$$3\mu_{\text{Cd}} + 2\mu_{\text{P}} \leq \Delta H_f(\text{Cd}_3\text{P}_2) \quad (3)$$

$$\mu_{\text{Ge}} + \mu_{\text{P}} \leq \Delta H_f(\text{GeP}) \quad (4)$$

to find the allowed range for μ_{Cd} and μ_{Ge} in CdGeP_2 . The electrons ionized upon forming a positively-charged defect join the Fermi sea so the formation energy increases by $q \epsilon_f$, where ϵ_f is the fermi energy which varies from 0 eV at the valence band maximum (VBM) of the host material to the band gap of the host [15]. Equations (2)-(4) were solved using the experimental values [16,17] of the formation energies for the binary phases Cd_3P_2 (-1.2 eV) and GeP (-0.3 eV), while a value of -1.5 eV, in the same range as other chalcopyrites [18] was used for CdGeP_2 .

The allowed range of chemical potentials μ_{Cd} and μ_{Ge} for CdGeP_2 and the binaries Cd_3P_2 and GeP are given in Fig. 1. There are three distinct chemical potential domains where CdGeP_2 can exist. For brevity we represent each region by one characteristic point: point A - (Cd rich; Ge poor); point B - (Cd rich; Ge-rich); and point C - (Cd poor; Ge rich). Figure 2 shows the formation energies of the intrinsic point defects Ge_{Cd} , V_{Cd} and V_{Ge} as well as substitutional defects Mn_{Ge} and Mn_{Cd} at the chemical potentials A, B and C of Fig. 1 as a function of the Fermi energy. The vertical dashed line denotes the GGA gap which is underestimated with respect to the experimental 1.72 eV gap. Transition points between charge states are indicated by solid circles. The defects can form acceptor states generating holes in the system [e.g. (-/0) or (2-/-)] or donor states that generate electrons [e.g. (0/+)]. We see that: (i) When CdGeP_2 is grown at point C (Cd-poor and Ge-rich), and to a lesser extent at point B (Cd-rich and Ge-rich), the favored substitution of Mn is on the Cd site. This substitution leads to a neutral charge state (no holes), thus to AFM. (ii) However, for n -type conditions (E_F near CBM) at point B, and at all E_F values at point A (Cd-rich; Ge-poor), the stablest site for Mn substitution is the Ge site. This substitution forms both single and double hole-producing acceptors, which can promote FM. However, under n -type conditions at point B, the charge state $q=-2$ is favored,

which has no holes and therefore promotes AFM. Analysis of the wavefunctions for different eigenvalues revealed that the Mn $3d$ levels are located 2-3 eV *below* the VBM and so one spin channel is fully filled (5 electrons). While formally Mn^{4+} would have a d^3 configuration, the existence of a fully occupied d^5 implies that two electrons are captured from the states near ϵ_f . The levels which are emptied correspond to the two acceptor state transitions taking place at 0.5 eV and 0.57 eV above E_{VBM} . (iii) Cadmium vacancies with the charge state $q=-2$ are easily formed (in n -type conditions) at points A and C. (iv) Ge vacancy is stable for n -type conditions of point A, though the charge state which has the lowest energy in these conditions has no holes. can promote ferromagnetism. (v) Ge-on-Cd antisite has high formation energy, and would therefore not have appreciable concentration.

Having identified the hole-producing centers that can yield ferromagnetism, we next examine the predicted solubilities of isolated Mn. Our calculated formation energies for $\text{CdGeP}_2:\text{Mn}$ and similar calculations for $\text{GaAs}:\text{Mn}$ show consistently lower values (for the appropriate chemical potentials) in the former case, predicting higher Mn solubility: the lowest formation energy of substituting a Ga atom with Mn in GaAs is 0.5 eV (under Mn-rich, Ga-poor conditions). In contrast, even in the worst-case scenarios, we find a value of ΔH_f 0.6 eV for Mn_{Cd} in CdGeP_2 under Cd-rich, Ge-poor conditions. For Mn_{Ge} we find $\Delta H_f \sim 0$ eV under Cd-poor, Ge-rich conditions.

Having established low substitution energies for Mn in CdGeP_2 we next see if Mn tends to cluster or not. We calculated the pairing energy, δ , of a pair relative to infinitely separated Mn atoms in the host, given, by $\delta = [E(2 \text{ Mn}) - E(0 \text{ Mn})] - 2[E(1 \text{ Mn}) - E(0 \text{ Mn})]$ where $E(n \text{ Mn})$ is the total energy of the supercell with n Mn atoms. A negative pairing energy would imply that the two Mn atoms would prefer to pair rather than stay far apart. The pairing energy for nearest neighbor Mn_{Cd} and Mn_{Ge} pairs were found to be +577 meV and +513 meV respectively for the unit cell considered, implying no clustering. On the other hand, Mn substitution of GaAs had a negative pairing energy, equal to -250 meV for Mn occupying nearest neighbor Ga sites. The corresponding energy for clusters of three or four Mn occupying the vertices of a tetrahedron surrounding a single As in GaAs was even more negative, indicating that the Mn atoms showed a tendency of forming clusters when introduced into GaAs . The Mn atoms doped into CdGeP_2 did not exhibit this tendency.

Having established that the isolated defects Mn_{Cd} , Mn_{Ge} and V_{Cd} have the lowest formation energy under certain experimental conditions and for some charge states the latter two are hole-producing (and therefore potentially ferromagnetism promoting), and that Mn_{Ge} pairs repel each other rather than cluster we now study various combinations of these point defects in search of stable, hole producing *complexes*. Two Mn atoms were introduced alongwith various intrinsic defects at various

positions of a 16 as well as 32 atom super cells of CdGeP₂ corresponding to 50% and 25% Mn respectively. The energies of the ferromagnetic and antiferromagnetic arrangements was computed for the fully-optimised super cell (*i.e* both cell external parameters as well as cell-internal atomic positions were relaxed). The formation energies of the defect complexes in the 32 atom unit cell are plotted in Fig. 3 as a function of μ_{Cd} in panel (a), and as a function of μ_{Ge} in panel (b). The nature of the magnetic ground state (A=AFM and F=FM) has been indicated in parentheses for the defect complex with the lowest energy. The vertical arrows denote the values of chemical potential for which there is a crossover in the type of defect with the lowest energy. We see that: (i) Under Ge-rich conditions, where *isolated* Mn prefers the Cd site (Fig. 2c), a pair of Mn atoms also prefers the Cd site (Fig. 3a), leading to an AFM ground state. For 25% Mn the antiferromagnetic state is lower in energy than the ferromagnetic state by 105, 19, 13 and 15 meV/Mn for Mn_{Cd}-Mn_{Cd} separations of 1st, 2nd, 3rd and 4th neighbors respectively. For the 50% doping, the energy difference changes from 124 to 23 meV/ Mn. The energy difference of 19 meV and 23 meV for 25% and 50% dopings for the second neighbor positions is in reasonable agreement with the difference of 21 meV and 35 meV obtained by earlier calculations [9]. (ii) Adding a Cd vacancy to the Mn_{Cd}-Mn_{Cd} pair lowers the energy for the Cd-poor range of Fig. 3a, but leaves the system as a whole antiferromagnetic. (iii) Under Cd-rich conditions, where *isolated* Mn prefers the Ge site (Fig. 2a), a pair of Mn atoms also prefers the Ge site (Fig. 3b), except at the very Ge-rich end. For 25% Mn the FM state is lower in energy than the AFM state by 111, 67 and 82 meV/Mn for Mn_{Ge}-Mn_{Ge} separations of 1st, 2nd and 3rd neighbors respectively. For the 50% Mn case, the ferromagnetic state is still stable by 131 and 158 meV/Mn for 1st and 2nd neighbors. The fact that the energy difference between the ferromagnetic and the antiferromagnetic states is quite large even when Mn atoms are at 3rd neighbor separation implies that the magnetic interactions are long-ranged in this case, unlike when Mn dopes the Cd site. (iv) The combination of Mn_{Cd}-Mn_{Ge} pairs is also ferromagnetic, being comparable in energy to when Mn replaces the Ge sites for certain chemical potentials of Fig. 3b.

In pure CdGeP₂ the valence electron configuration is $a^2t_p^6$, where p denotes the dominant character of the level. This reflects the fact that Ge contributes 1 electron to each of the 4 bonds with P, Cd contributes $\frac{1}{2}$ electron and P contributes $\frac{5}{4}$ electrons; the GeP₄ tetrahedron transfers one electron to the CdP₄ tetrahedron, through the bridging P. The electronic structure of a transition metal substituting a cation site in a semiconductor can be described by the hybridization between the orbitals of the transition metal ion and the anion dangling bonds formed from the cation vacancy in the host semiconductor [2]. Figure 4 shows this for Mn_{Ge} in CdGeP₂. The levels

with t_\uparrow character on Mn (left) hybridize with the levels with the same symmetry on the Ge-vacancy dangling bond (right), thus forming a bonding "crystal field resonance" (CFR) $t_{CFR\uparrow}$ located deep in the valence band with dominant Mn character, and antibonding "dangling bond hybrid" (DBH) $t_{DBH\uparrow}$ with dominantly p character. A similar hybridization of the down-spin levels results in the down-spin counterparts of the CFR and DBH levels. The CFR level with e symmetry exists too. These e_{CFR} , t_{CFR} levels can hold 5 electrons. When Mn is substituted on the Ge site, 4 of its 7 valence electrons replace those of Ge, leaving 3 electrons to occupy the $t_{CFR\uparrow}$ $e_{CFR\uparrow}$. However, since t_{DBH} is higher in energy than $e_{CFR\uparrow}$, two electrons move into $e_{CFR\uparrow}$, leading to ($e_{CFR\uparrow}^2 t_{CFR\uparrow}^3$) consequently, two holes (empty circles in Fig. 4) are generated in the DBH levels. The intraatomic exchange splitting on the Mn atoms is large, $\sim 0.6-0.7$ eV [19], and what is unusual here is that it induces a large negative (0.8-1.0 eV) exchange splitting on the DBH levels which have dominantly P p character. The direction of the exchange splitting on the DBH (spin-down below spin-up) is opposite to the direction of exchange splitting on the CFR levels, and this can be understood by simple tight-binding arguments. If the up-spin states on both the DBH and CFR are occupied, then the energy gain as a result of hybridization is small and comes from the single electron occupying the down spin DBH levels. However, if the up spin states on the CFR and the down spin states on the DBH are occupied, the energy gain as a result of hybridization is huge and there are contributions from both up and down spin channels. Hence the configuration in which the up spin levels on the CFR and the down spin levels on the DBH are occupied is the ground state of the system. A similar hybridization-induced antiferromagnetic coupling was earlier proposed to explain the high Curie temperature observed in another ferromagnet in which the magnetic Fe atoms are separated by nonmagnetic Mo atoms [20]. In the inset of Fig. 4 we show the contributions to the total DOS from the up-spin states as well as the Mn d states in a small energy window near the fermi energy. The states are found to be strongly spin-polarized, with just 25% Mn d character from the two Mn atoms present in the 32 atom super cell considered here. As a result of the large exchange splitting induced on the DBH states, the downspin DBH bands are energetically degenerate with the dominantly P p bands. The strongly polarised as well as delocalised down spin DBH band we believe is responsible for the long-ranged magnetic interactions, and, consequently the room temperature ferromagnetism found in Mn doped CdGeP₂.

We thank D.D. Sarma for useful discussions. This work was supported by the U.S. DOE under contract no. DE-AC36-99-G010337.

- [1] T. Dietl *et al.*, Science **287**, 1019 (2000); T. Dietl, J. Appl. Phys. **89**, 7437 (2001).
- [2] A. Zunger in *Solid State Physics* **39**, 275 (Academic Press, New York, 1986).
- [3] H. Munekata *et al.*, Phys. Rev. Lett. **63**, 1849 (1989).
- [4] J.K. Furdyna and J. Kossut, *Semiconductors and semimetals* **25**, (Academic Press, San Diego, 1988).
- [5] J. Schneider *et al.*, Phys. Rev. Lett. **59**, 240 (1987).
- [6] G.A. Medvedkin *et al.*, Jpn. J. Appl. Phys., Part 2 **39**, L949 (2000).
- [7] J.E. Jaffe and A. Zunger, Phys. Rev. B **30**, 741 (1984).
- [8] S.H. Wei and A. Zunger, Phys. Rev. B **35**, 2340 (1987).
- [9] Yu-Jun Zhao, W.T. Geng, A.J. Freeman and T. Oguchi, Phys. Rev B **63**, 201202(R) (2001).
- [10] S.B. Zhang, S.H. Wei and A. Zunger, Phys. Rev. Lett. **78**, 4059 (1997); S.B. Zhang, S.H. Wei, A. Zunger and H. Katayama-Yoshida, Phys. Rev. B **57**, 9642 (1998).
- [11] The pseudopotential plane-wave method [12] using GGA PW91 ultrasoft pseudopotentials as implemented in VASP [13] was used for the calculations. Cutoff energies of 16.7 Ry (28.2 Ry) and 15.9 Ry (20.2 Ry) were used for the plane-wave (augmentation charge) for the calculations with and without Mn respectively. A Monkhorst-Pack k-points grid of 4x4x2, 2x4x2 and 2x2x2 was used for the calculations involving 16, 32 and 64 atoms.
- [12] J. Ihm, A. Zunger and M.L. Cohen, J. Phys. C:**12**, 4409 (1979).
- [13] G. Kresse and J. Furthmüller, Phys. Rev. B. **54**, 11169 (1996); G. Kresse and J. Furthmüller, Comput. Mat. Sci. **6**, 15 (1996).
- [14] P. Villars and J.L. Calvert, *Pearson's Handbook of Crystallographic Data for Intermetallic Phases* (ASM International, Materials Park, 1991).
- [15] The GGA calculated gap was found to be 0.65 eV.
- [16] Editors Wagman *et al.*, Vol. 11, *NBS tables of chemical thermodynamic properties*, (ACS and AIP for the National Bureau of Standards, 1982).
- [17] The calculated formation energies were -1.3 eV, +0.33 eV and -0.93 eV for Cd₃P₂, GeP and CdGeP₂. The use of the calculated formation energies instead of the experimental ones does not change the conclusions of our work.
- [18] L.I. Berger, *Semiconductor Materials* (CRC press, New York, 1997), p.230.
- [19] P. Mahadevan, N. Shanthi and D.D. Sarma, J. Phys. Condens. Matter **9**, 3129 (1997).
- [20] D.D. Sarma *et al.*, Phys. Rev. Lett. **85**, 2549 (2000).

FIG. 1. The range of Cd and Ge chemical potentials where CdGeP₂, GeP and Cd₃P₂ are stable.

FIG. 2. The formation energies of different charge states of isolated defects calculated as a function of fermi energy in a 64 atom cell of CdGeP₂ for three chemical potentials: A, B and C. The vertical dashed line denotes the calculated GGA band gap. Solid circles denote transition energies between charged states.

FIG. 3. The formation energies as a function of (a) Cd (b) Ge chemical potentials calculated for complex defects in a 32 atom cell of CdGeP₂. The magnetic ground state (A=AFM, F=FM) for the lowest energy state is indicated in parentheses. The vertical arrows denote the value of chemical potential for which there is a crossover in the lowest energy defect type.

FIG. 4. The energy level diagram of Mn_{Ge} in CdGeP₂. The energy of the levels are indicated in brackets. The inset shows the contributions to the total DOS in the energy interval -0.5 eV to 0.5 eV from the up spin states as well as Mn 3d calculated for 2 Mn_{Ge} in a 32 atom unit cell of CdGeP₂.

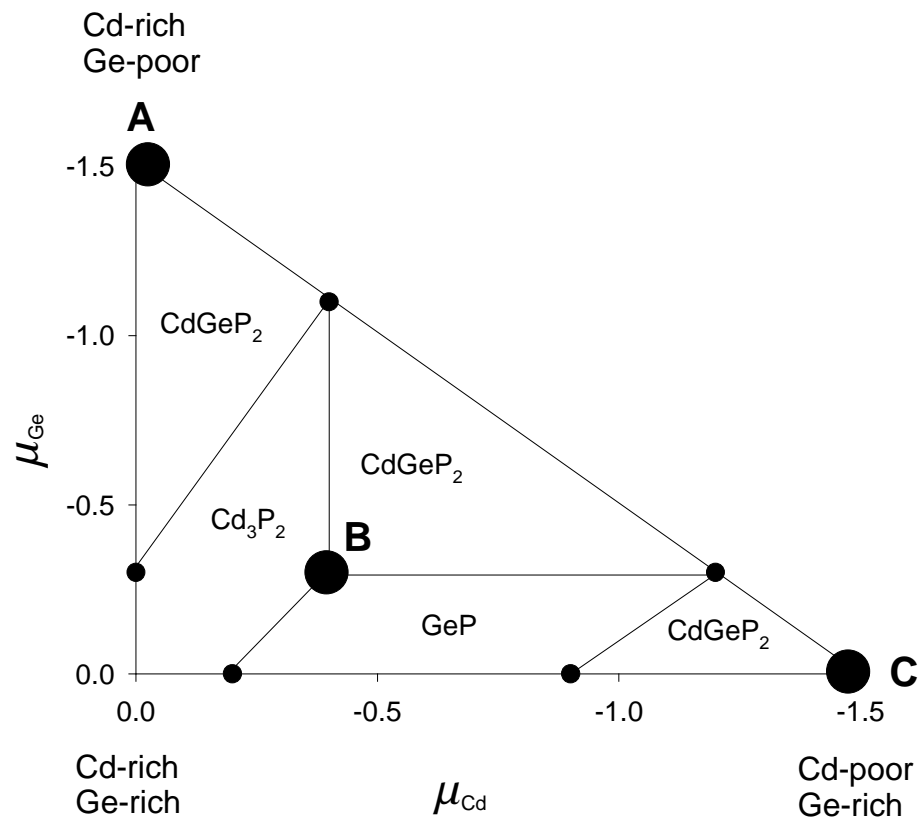


Fig. 1

Mahadevan *et al.*

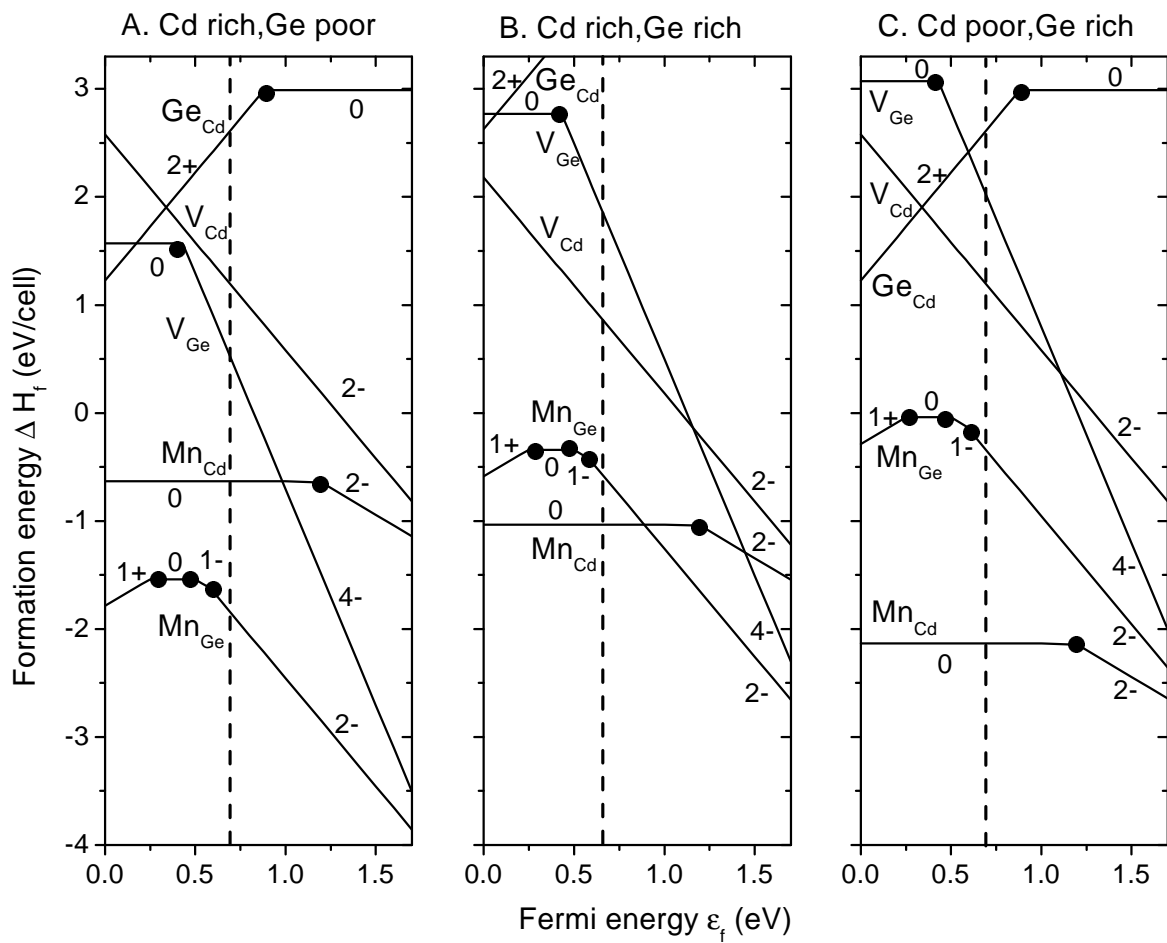


Fig.2
Mahadevan *et al.*

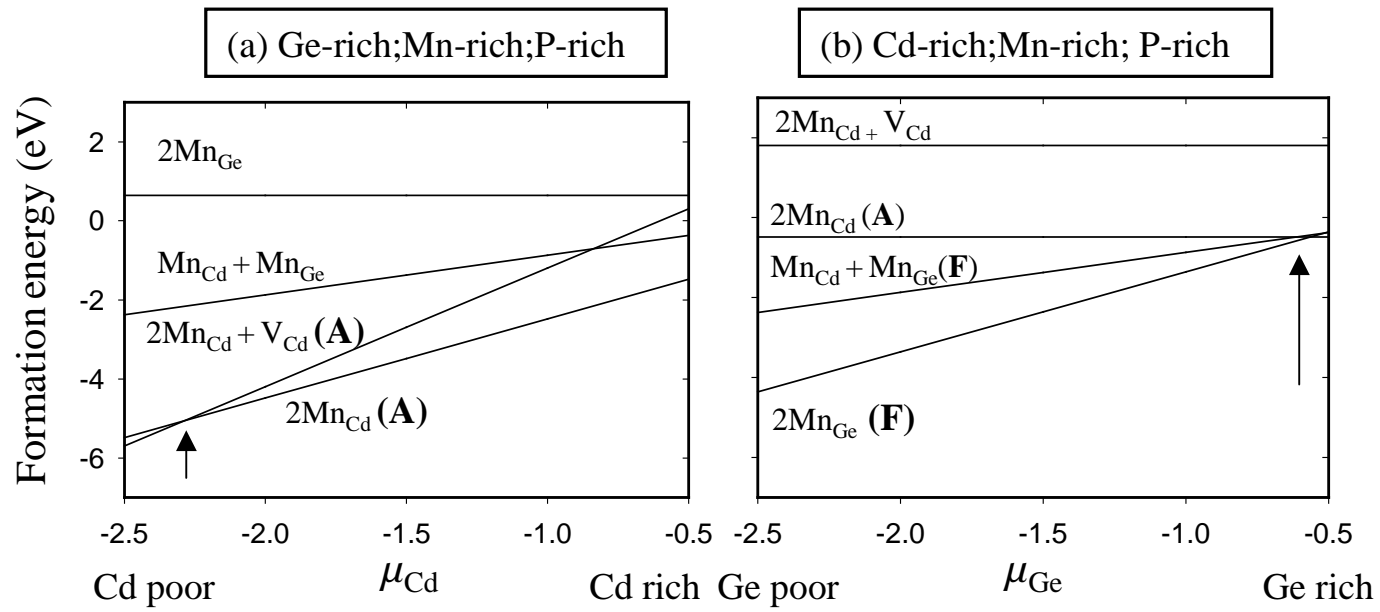


Fig.3

Mahadevan *et al.*

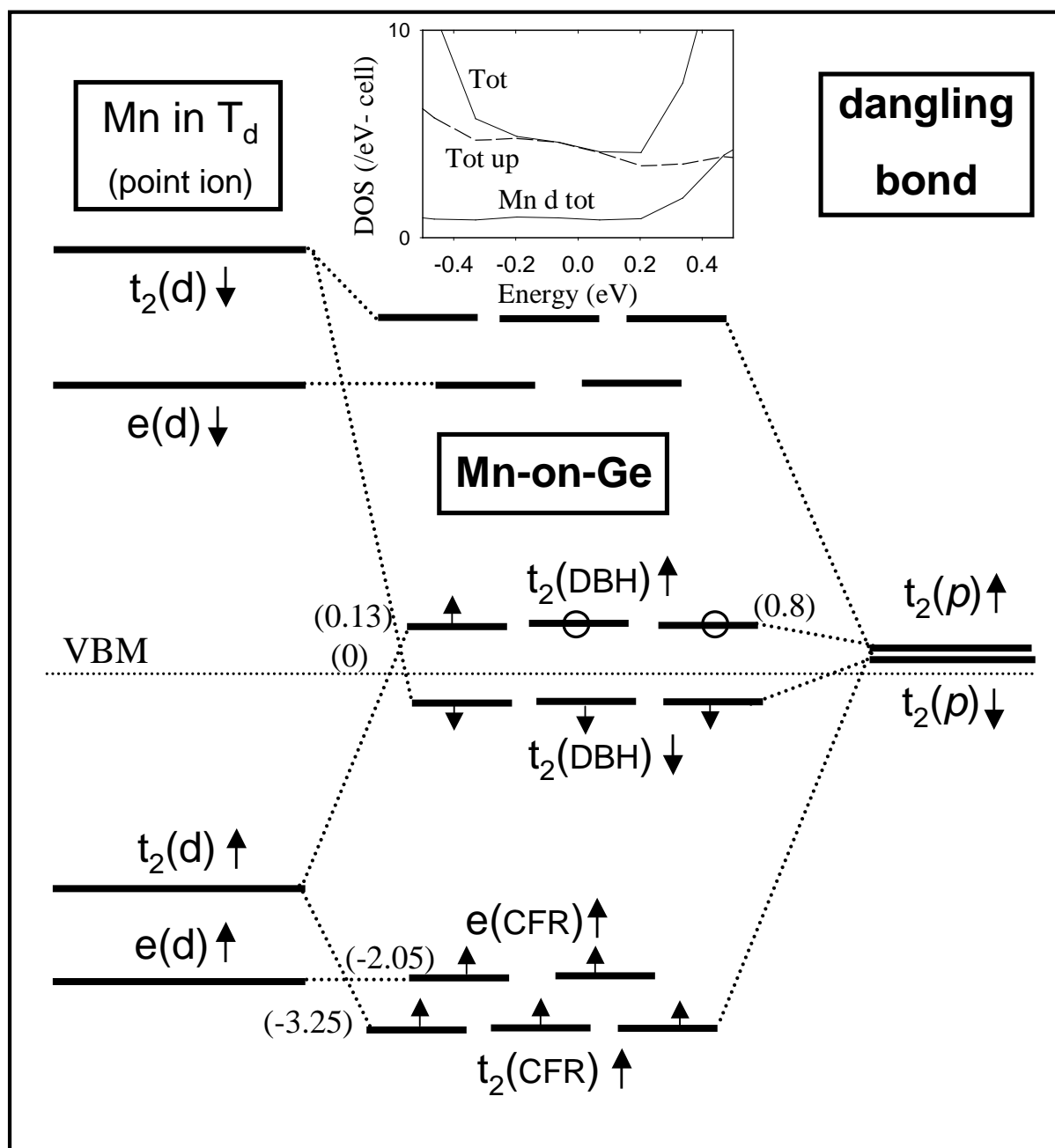


Fig.4

Mahadevan *et al.*